Why Does Argon Bind to Deuterium? Isotope Effects and Structures of $Ar \cdot H_5O_2^+$ Complexes

Laura R. McCunn,[†] Joseph R. Roscioli,[†] Ben M. Elliott,[†] Mark A. Johnson,*[,†] and Anne B. McCoy*[,‡]

Department of Chemistry, Yale University, New Haven, Connecticut 06520, and Department of Chemistry, The Ohio State University, Columbus, Ohio 43210

Received: March 12, 2008; Revised Manuscript Received: April 11, 2008

Recently, we reported the spectrum of $Ar \cdot D_4HO_2^+$ [McCunn; et, al. *J. Phys. Chem. B* **2008**, *112*, 321], and here, we extend that work to include the $Ar \cdot H_4DO_2^+$ isotopologue in order to explore why the Ar atom has a much greater propensity for attachment to a dangling OD group than it does for OH, even when many more of the latter binding sites are available. Calculated (MP2/6-311+G(d,p) level of theory/basis) harmonic frequencies reproduce the observed multiplet patterns of OH and OD stretches and confirm the presence of various isomers arising from the different Ar binding sites. The preferential bonding of Ar to OD is traced to changes in the frequencies of the wag and rock modes of the $H_5O_2^+$ moiety rather than to shifts in the oscillator that directly binds the Ar atom.

I. Introduction

An important benchmark for our theoretical understanding of intermolecular interactions is to recover the relative stabilities of conformers formed by weakly bound complexes.[1–3] The focus in this work is on attachment of an argon atom to equivalent hydroxyl groups in the Zundel ion, $H_2O \cdot H^+ \cdot OH_2$,[4] in situations where this equivalence is broken by replacement of one or more hydrogen atoms with deuterium. In that case, the overall zero-point vibrational energies (ZPE) for the isomers corresponding to Ar attachment to dangling H or D atoms will be different, even though the potential energy describing the argon attachment to OH is identical to that of OD. Which configuration is most stable is often subtle because it involves a competition between the decreasing frequency of the OH stretch and the increasing frequencies of the slower wag and rock motions. Here, we determine the distribution of Ar atoms in H and D binding sites in the $Ar \cdot H_4DO_2^+$ and $Ar \cdot D_4HO_2^+$ complexes using vibrational spectroscopy and then deduce which modes are causing this fractionation by using theoretical calculations to probe the origins of their different ZPE values.

The $H_5O_2^+$ ion has been the subject of intense study in recent years.[5–9] In its equilibrium structure, the excess proton is located equidistant between the two oxygen atoms of the two flanking water molecules. The Ar attaches to any one of the four OH bonds in the water molecules, resulting in four equivalent minima on the potential surface, with one of these minimum-energy structures[8] presented in Figure 1. Isotope fractionation effects in the Ar−Zundel complex were first discovered accidentally in the course of our recent report analyzing the isotope dependence of the various bands determined by applying Ar predissociation spectroscopy to the $Ar \cdot D_4HO_2^+$ isotopologue.[9] That paper focused on the cause of band doubling in the transitions associated with the shared H in the Zundel ion, and the isomer with H in the shared position was found to be the dominant $Ar \cdot D_4HO_2^+$ species formed in the jet. This preference was anticipated in an earlier study by Buch and coworkers,[10] who calculated the isomer's energy to be ~170 cm^{-1} below that of the isomer with D in the bridging position. There was, however, a minor contribution in our spectrum from the higher energy $D_4HO_2^+$ species with a bridging D atom. Interestingly, although this isomer presents both H and D atoms in the dangling positions, the Ar atom was only rarely found to attach to the H atom. This observation led to the present study where we examine the cause for preferential Ar attachment to exposed OD binding sites.

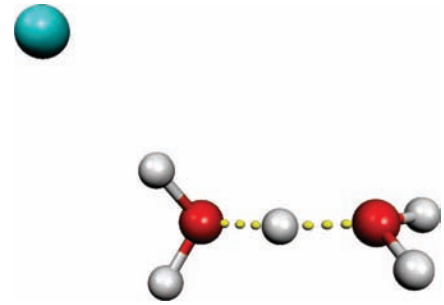

Figure 1. Structure of the $Ar \cdot H_5O_2^+$ complex as calculated at the MP2/6-311+G(d,p) level of theory.

The isomers that are differentiated according to the (H versus D) location of an attached Ar atom are particularly interesting because interconversion within this class is efficiently mediated by the bimolecular displacement process in the jet[11,12]

$$Ar \cdot D{-}R{-}H + Ar \rightarrow Ar \cdot H{-}R{-}D + Ar \qquad (1)$$

where R denotes the spectator constituents of the Zundel ion. As such, the population distribution among these isomers is much more likely to reflect the ambient translational temperature of the jet,[13,14] and consequently that of the low-frequency modes of the cluster, than are species separated by large barriers. The latter class, for example, comprises the isomers derived from fractionation of the H and D atoms into the bridging position of the Zundel ion.

* Corresponding authors. E-mail: M.A.J., mark.johnson@yale.edu; A.B.M., mccoy@chemistry.ohio-state.edu.
[†] Yale University.
[‡] The Ohio State University.

10.1021/jp802172q CCC: $40.75
Published on Web 06/18/2008

Our intent is to explore the topology of the argon attachment landscape in a comparative spectroscopic study of the complementary $Ar \cdot D_4HO_2^+$ and $Ar \cdot H_4DO_2^+$ isotopomers. Isotopic fractionation under quasi-equilibrium conditions must reflect ZPE effects; therefore, to understand the relative energies and spectral signatures of the various species, we have performed harmonic calculations for the partially deuterated complexes. Earlier calculations by Jordan[8] as well as by Bosch and coworkers[15] established that the MP2 level of theory reproduces the simpler OH stretching region of the $Ar \cdot H_5O_2^+$ vibrational spectrum (as opposed to the lower energy bands arising from the intracluster bends and displacements of the bridging proton) with scaled harmonic frequencies. Here, we consider several electronic structure methods and basis sets in order to understand the observed trends in Ar attachment to the partially deuterated isotopologues of the Zundel ion.

II. Experimental Methods

Vibrational predissociation spectra were recorded with the Yale double-focusing, tandem time-of-flight photofragmentation spectrometer described previously.[16] Cluster ions were formed by ionizing a supersonic expansion with a pulsed (50 μs) 1 keV electron beam. A mixture of H_2O/D_2O vapor was entrained into an Ar/H_2O expansion by using a separate pulsed valve located on the low pressure side of the expansion.[17] The Ar-tagged complexes were then likely formed by Ar-mediated condensation.

$$H_3O^+ \cdot Ar_n + HDO \rightarrow H_2O \cdot H^+ \cdot ODH \cdot Ar + (n-1)Ar \quad (2)$$

Photoexcitation was carried out by using a Nd:YAG-pumped OPO/OPA (Laser Vision) with a KTP oscillator and parametric conversion using KTA. Spectra typically resulted from the summation of 10−15 individual scans and are reported as photofragment yield, normalized for the laser output power at each wavelength.

III. Computational Details

All calculations were performed by using the Gaussian03 program package.[18] We calculated the equilibrium geometry, Cartesian force constants, and dipole derivatives at the HF, DFT (by using the B3LYP functional), and the MP2 levels of theory, with 6-311+G(d,p), aug-cc-pvdz, and aug-cc-pvtz basis sets. The final results are independent of the level of theory or basis used, and we report those results acquired by using a 6-311+G(d,p) basis. Once we obtained this information for $Ar \cdot H_5O_2^+$, we used the force constants and dipole derivatives to construct the mass-weighted Hessian matrix and dipole derivatives for all of the remaining isotopologues. To make direct comparisons with the experimental spectra, which have been divided by the laser power, we divide the calculated intensities by the frequencies of the transitions. In addition, to account approximately for anharmonicity, the scaling factors 0.9460 (for OH stretches) and 0.9574 (for OD stretches) were used throughout the study. These factors were obtained to maximize the agreement with the experimental spectra for $Ar \cdot H_5O_2^+$ and $Ar \cdot D_5O_2^+$.

IV. Results

A. Experimental Spectra. An overview of the predissociation spectra for four Ar-tagged isotopologues, $H_5O_2^+$, $D_5O_2^+$, $H_4DO_2^+$, and $D_4HO_2^+$, is presented in Figure 2. All spectra were reported earlier,[9] except that of $Ar \cdot H_4DO_2^+$ (trace c). As discussed previously, the greater than factor-of-three difference

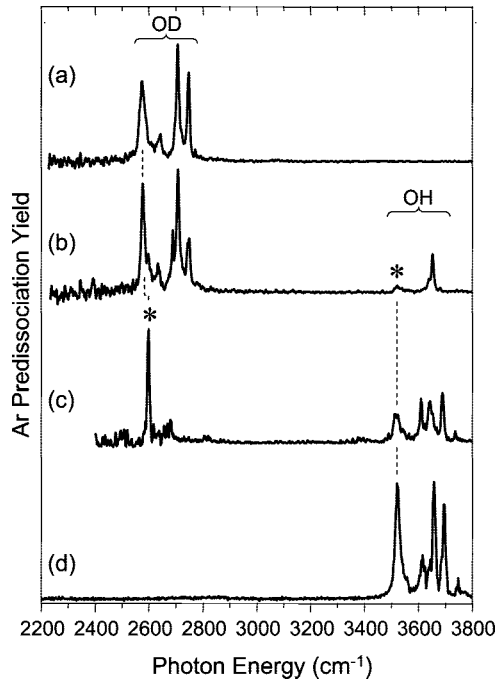

Figure 2. Predissociation spectra for (a) $Ar \cdot D_5O_2^+$, (b) $Ar \cdot D_4HO_2^+$, (c) $Ar \cdot H_4DO_2^+$, and (d) $Ar \cdot H_5O_2^+$. Traces a, b, and d are reproduced with permission from *J. Chem. Phys. B* **2008**, *112,* 321−327. The asterisks and dashed lines track the appearance of bands associated with Ar-bound OH and Ar-bound OD.

in the frequencies of the dangling OH stretch compared to those of the shared H causes the isomer with a lighter H atom in the bridging position to occur lowest in energy. For a series of Zundel ion isotopologues, Buch and co-workers[10] estimated the bridging H isomer to lie 170 cm^{-1} below that with bridging D based on DMC calculations which employed the OSS3 potential;[19] DMC calculations based on the HBB potential[20] for $H_5O_2^+$, which were carried out in the course of this work, refined this prediction and yielded a smaller value of 120 cm^{-1}.[9]

The intrinsic splitting pattern of high-frequency stretches for the homogeneous isotopologues consists of four distinct features, and these are readily assigned with the scaled harmonic values arising from the minimum-energy structure shown in Figure 1. The accuracy of this treatment is illustrated in Figure 3, which presents expanded views of the observed (upward peaks) and calculated (downward peaks) OH and OD stretching bands for $Ar \cdot D_5O_2^+$ and $Ar \cdot H_5O_2^+$ in the left and right panels, respectively. The small feature, highest in energy at ~3750 cm^{-1} (‡), is commonly observed in cationic complexes involving water[21] and very likely results from a combination band involving frustrated internal rotation of one of the water molecules. Within the OD and OH subgroups, the strong peak that is lowest in energy is associated with the oscillator bound to the Ar atom, and its motion is largely decoupled from the other dangling atoms. The companion atom on the Ar-bound water molecule accounts for the next strongest peak, which splits the coupled symmetric and asymmetric stretching fundamentals arising from the free water molecule remote from the Ar atom.

When only one D or H atom is present in an outer position, the propensity for Ar to bind to that unique atom is immediately clear from the intensity of the resulting red-shifted signature feature. With this in mind, qualitative comparison between the minor isotope stretching bands in the $Ar \cdot D_4HO_2^+$ and $Ar \cdot H_4DO_2^+$ spectra (Figure 2b,c, respectively) dramatically illustrates the different solvation behavior in the two cases.

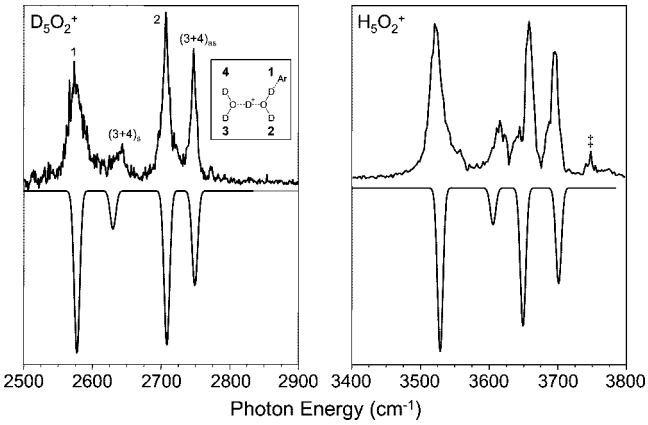

Figure 3. Comparison of calculated [MP2/6-311+G(d,p)] (downward trace) and predissociation (upward trace) spectra for $Ar \cdot H_5O_2^+$ and $Ar \cdot D_5O_2^+$. The calculated OH stretch frequencies are scaled by 0.9460, whereas a factor of 0.9574 is applied to the OD stretch frequencies. The vibrational assignments are referenced by the dominant normal mode displacements associated with the numbered OD bonds in the inset. The vibrations on the free water molecule are collective symmetric $(3 + 4)_s$ and asymmetric $(3 + 4)_{as}$ motions, whereas the Ar atom acts to decouple these vibrations for atoms 1 and 2. The peak labeled ‡ is assigned to a combination band, most likely involving frustrated internal rotation of the complex.

Specifically, when only one H is present, its free OH stretching pattern is dominated by a single band at 3653 cm^{-1}, about 130 cm^{-1} to the blue of the Ar-bound stretch (3519 cm^{-1}, asterisk in Figure 2b). On the other hand, when only one D is available in an outer position, the OD-Ar band is now dominant (asterisk in Figure 2c), with only a minor contribution from the higher-energy, unsolvated OD stretch.

At first glance, the preference of Ar binding to D over H is perplexing, because this attachment gives rise to a substantial (100 cm^{-1}) red shift in the stretching transition, and it is precisely the large red shift in the exterior versus bridging position that leads to strong fractionation of the lighter H atom to be shared in the $H_5O_2^+$ core ion. In the case of Ar-attachment, the observed preference is for D to be shared between O and Ar; therefore, other effects must be at play.

B. Harmonic Analysis. Quantitative analysis of the relative isomer abundances in the mixed-isotope species requires disentangling the contributions of their distinct spectral patterns in both the OH and OD regions. The accuracy of the scaled harmonic calculations in recovering the stretching bands in the homogeneous isotopomers is thus important, as it validates our ability to assign correctly the overlapping band patterns.

In the $Ar \cdot D_4HO_2^+$ and $Ar \cdot H_4DO_2^+$ isotopomers where the unique atom occupies a dangling position (i.e., $D_2O \cdot D^+ \cdot ODH$ and $H_2O \cdot H^+ \cdot OHD$), there are four distinct possibilities for Ar attachment, and each is distinguishable by the frequency of its OH or OD stretch. Table 1 presents the scaled OH-stretch frequencies and corresponding intensities for the four isomers of $Ar \cdot D_4HO_2^+$ and the analogous OD-stretch frequencies for $Ar \cdot H_4DO_2^+$. In this table, we label each isomer by the position of the unique (H/D) atom relative to the Ar atom [binding directly to Ar (Ar-bound), unbound and residing in an Ar-bound HOD molecule (Ar end), or residing opposite the Ar-bound water molecule (free end)]. The reported band intensities are the calculated intensity (km/mol) divided by the transition frequency for direct comparison with the experimental action spectra and are scaled so that the fundamental of the most intense, Ar-bound OH/OD stretch is set to unity.

Simulation of the observed spectra requires convolution of the contributions from each of the isomers, weighted according to their thermal population distribution at the effective translational temperature describing their formation (eq 1). Overall, this includes first considering the population containing a bridging H versus a bridging D in the core Zundel ion and then determining the relative populations of the four distinct Ar-based isomers. In this first analysis, we focus on the harmonic ZPEs to evaluate the general trends, which are included in Table 1. As mentioned above, the harmonic ZPEs of the isomers of $Ar \cdot H_4DO_2^+$ and $Ar \cdot D_4HO_2^+$ indeed strongly favor those with bridging H atoms in the core ion. Of the four remaining $Ar \cdot D_4HO_2^+$ isomers that arise from the different arrangements of Ar binding to a core with a bridging D, the one in which the single H atom resides in the Ar-bound position has the highest ZPE by roughly 30 cm^{-1}, whereas that with deuterium in the Ar-bound position occurs lowest in energy. These energetics are consistent with the observed propensity for the Ar atom to bind to a dangling OD group. On the other hand, the lowest-energy isomer of $Ar \cdot H_4DO_2^+$ has the unique deuterium atom in the Ar-bound position. A full list of calculated harmonic frequencies is available in the Supporting Information. Notably, the same trend is obtained for a variety of basis sets, aug-cc-pvdz, aug-cc-pvtz, and 6-311+G(d,p), and at the HF, MP2, and B3LYP levels of theory. The results presented are from the MP2/6-311+G(d,p) calculations.

Figure 4 presents a comparison of the $Ar \cdot D_4HO_2^+$ and $Ar \cdot H_4DO_2^+$ experimental spectra to the calculated harmonic bands for each of the possible isomers. In the case of $D_4HO_2^+$ (traces c and d), the predicted spectrum of the energetically favored bridging-H isomer does not account for all of the bands in the experimental data. There are clear contributions from the four shared-D isomers, and the relative intensities of their vibrational bands will be significantly affected by the temperature of the cluster ensemble. To gauge whether a Boltzmann-weighted distribution of isomers can recover the qualitative character of the observed spectra, the scaled harmonic peaks for the four isomers (of the $D_2O \cdot D^+ \cdot OHD$ and $H_2O \cdot H^+ \cdot OHD$ isotopomers) were convoluted with Gaussians (10 cm^{-1} FWHM) at the expected jet translational temperature of 25 K.[22] The overall patterns are compared in Figure 4, illustrating that the observed bands are reproduced quite well, especially the striking disparity between Ar solvation of the dangling H in $D_2O \cdot D^+ \cdot ODH$ (Figure 4d) and the dangling D in $H_2O \cdot H^+ \cdot OHD$ (Figure 4a). This analysis also allows us to assign the various bands to specific isomers, which yields an exquisitely detailed picture of Ar-induced symmetry-breaking and perturbation of the solvated Zundel ion. For example, examination of the $Ar \cdot D_4HO_2^+$ spectra (Figure 4c) reveals that, although many of the bands overlap with the predicted shared-H isotopomer bands, the free-end isomers ($Ar \cdot D_2O \cdot D^+ \cdot OHD$) account for the sharp shoulder at 2688 cm^{-1}.

We anticipate that this isotope fractionation effect can be developed as a transferable and spectroscopy-based method in which to compare the temperatures of the clusters prepared in various ion sources and in different laboratories. The focus here, however, is to identify the band patterns and underlying origin of the effect. Given the approximations used in obtaining the calculated spectra, it is not yet appropriate to assign a quantitative temperature to the experimental spectra on the basis of our analysis. It is nonetheless useful to note that the detailed spectral patterns revealed here can be immediately used to indicate relative temperatures at different experimental conditions and will ultimately index the temperature in these (and other) studies once the thermochemistry of the isotopomers becomes available. A fruitful direction for this work is thus to obtain accurate ZPE

TABLE 1: Scaled Frequencies and Relative Intensities of the OH Stretch in $Ar \cdot D_4HO_2^+$ and the OD Stretch in $Ar \cdot H_4DO_2^+$

	$Ar \cdot D_4HO_2^+$			$Ar \cdot H_4DO_2^+$		
H/D position	OH-stretch frequency (cm^{-1})[a]	relative intensity	relative ZPE (cm^{-1})	OD-stretch frequency (cm^{-1})[b]	relative intensity	relative ZPE (cm^{-1})
free end	3702	0.338	−28	2657	0.322	29
free end	3695	0.348	−26	2653	0.337	26
Ar end	3676	0.404	−12	2640	0.399	13
Ar-bound	3590	1.000	0	2580	1.000	0

[a] OH-stretch frequencies have been multiplied by 0.9460. [b] OD-stretch frequencies have been multiplied by 0.9574.

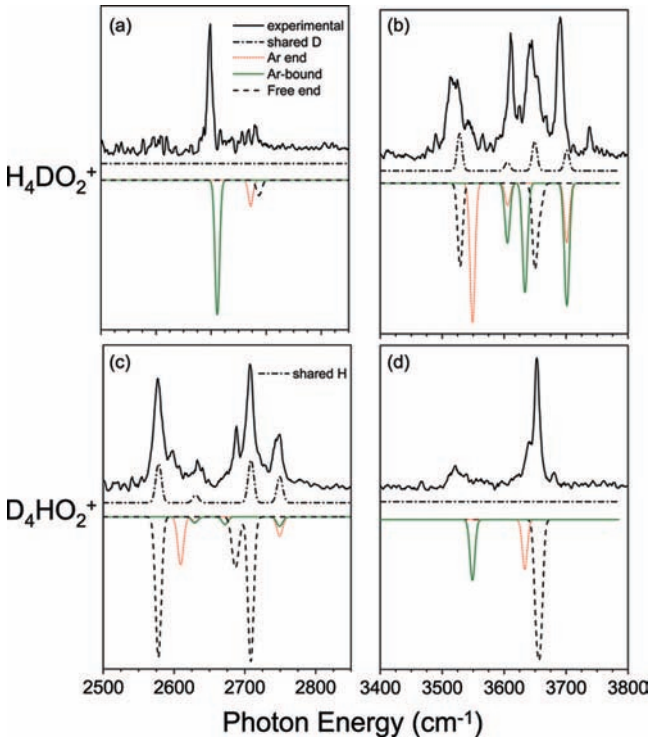

Figure 4. Comparison of calculated [MP2/6-311+G(d,p)] and predissociation spectra for $Ar \cdot H_4DO_2^+$ and $Ar \cdot D_4HO_2^+$. The calculated OH stretch frequencies are scaled by 0.9460, whereas the OD stretch frequencies are multiplied by 0.9574. The upward traces show the experimental data and the calculated spectra for the isotopomers with the unique isotope in the bridging position. The downward traces display calculated spectra for the isomers with the unique atom in an external position, classified by the position of the Ar atom. The free-end isomer has the Ar atom bound to the H_2O or D_2O molecule. The Ar-bound label indicates that the Ar is attached to the unique atom, and Ar-end means that the Ar is attached to the HOD molecule but not the unique atom itself.

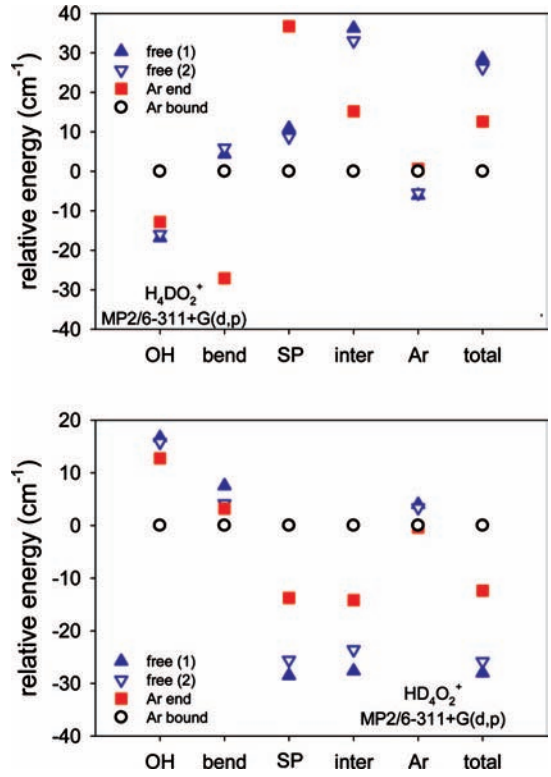

Figure 5. Decomposition of the $Ar \cdot H_4DO_2^+$ and $Ar \cdot D_4HO_2^+$ ZPEs, calculated at the MP2/6-311+G(d,p) level of theory/basis. Energies were calculated for the four isomers in which the unique isotope resides in the non-bridging position in the core Zundel ion. These are labeled according to whether the unique D/H atom is unbound [free (1) and free (2)], has an attached Ar (Ar-bound), or is an unbound H/D residing in the Ar-bound HOD molecule (Ar end). The results are categorized by the different classes of vibrational modes: OH stretches (OH), H_2O bends (bend), motions of the shared proton (SP), intermolecular vibrations (inter), and motions of the Ar atom (Ar).

values by using either anharmonic calculations or direct measurement of the spectral patterns in a temperature-controlled ion trap.[23,24]

C. Contributions to the Relative ZPEs. Because the experimental band pattern can be reproduced in the context of harmonic zero-point differences at reasonable temperatures for a free jet, we can use the calculations to extract what factors contribute to the energy ordering. To investigate this, we divide the 18 normal modes into five groups. Four modes correspond to OH or OD stretches; two derive from water bends, three are from motions of the shared H or D atom, six are low frequency modes that correspond to the O−O stretch and the wags, rocks, and torsions of the water molecule, and finally, three modes correspond to the intermolecular Ar motions. The relative values of the contributions of these five groups of modes to the overall ZPEs are plotted in Figure 5. It is clear that the trends in the ZPEs of the OH/OD stretches (denoted OH), water bends (bend), and Ar motions (Ar) do not match those of the total ZPE. Rather, the contributions from the low-frequency, intermolecular vibrations (denoted inter in Figure 5) mimic the overall ZPE, in terms of both the energy ordering and the magnitude.

The above results clearly illustrate that the observed relative energies of the various isomers reflect changes not in the frequencies associated with the separate water molecules or the Ar atom, but with the other, lower-frequency motions of the ion−Ar complex. Specifically, the introduction of the Ar atom leads to partial confinement of the motion of the wags, rocks, and torsions, thereby leading to an increase in ZPE. This increase will be larger if a H atom is involved in these motions.

It is useful to consider the conclusions of this work in the context of the behavior of other water complexes. More than 20 years ago, Engdahl and Nelander showed that in the case of deuterated water dimer, the deuterium-bound conformers of $H_2O \cdot D_2O$ or $(HOD)_2$ have lower ZPEs than the H-bound

conformers. As in the present work, they attributed this to changes in frequencies in the intermolecular degrees of freedom upon H-bond formation.[25] Likewise, in the case of $I^-\cdot DOH$, for example, the D atom is preferentially in the bound position, whereas in $F^-\cdot HOD$, the H atom is in the bound position.[26] More recently, we have found that $Cl^-\cdot DOH$ behaves like the I^- complex.[27] The OH-stretch frequency of the halide-bound OH bond in $F^-\cdot H_2O$ is considerably lower than the OH-stretch frequency in water. This large difference in ZPE is the driving force for the H being in the shared position. This is analogous to the situation of the shared H in Zundel. In $I^-\cdot H_2O$, the difference between the OH-stretch frequencies is small, and it is the dependence of the lower frequency in-plane and out-of-plane bends upon the location of the D atom that determines the energy ordering of the two isomers.[26] This is entirely consistent with what we observe here in understanding the preference for a D atom to be in the Ar-bound position in the mixed isotopologues of the Ar−Zundel complex.

V. Summary

Ar-predissociation spectra are reported in the OH and OD stretching regions for the $H_4DO_2^+$ and $D_4HO_2^+$ isotopologues of the Zundel ion, where the resulting bands are analyzed in the context of contributions from isotopomers with bridging H and D atoms in the Zundel core ion, as well as the isomers that arise from various locations of Ar-atom attachment among the four dangling H/D atoms. Harmonic analysis recovers the observed band patterns quite accurately and, in turn, confirms that it is much more likely for an Ar atom to bind to an available OD group rather than to OH, even when many more of the latter are available. Consideration of the relative contributions to the ZPEs of each isomer reveals that the observed isotope fractionation arises from the effect of Ar attachment on the low-frequency intermolecular motions of the proton-bound complex, as opposed to the behavior that would be anticipated from the strong red-shift in the local oscillator to which the Ar attaches.

Acknowledgment. M.A.J. and A.B.M. thank the Chemistry Division of the National Science Foundation for support of this work.

Supporting Information Available: A list of the MP2/6-311+G(d,p) frequencies and intensities for the 10 deuterated $Ar\cdot H_5O_2^+$ complexes is provided. This material is available free of charge via the Internet at http://pubs.acs.org.

References and Notes

(1) Hutson, J. M. *J. Chem. Phys.* **1992**, *96*, 6752.
(2) Rohrbacher, A.; Williams, J.; Janda, K. C. *Phys. Chem. Chem. Phys.* **1999**, *1*, 5263.
(3) McCoy, A. B.; Darr, J. P.; Boucher, D. S.; Winter, P. R.; Bradke, M. D.; Loomis, R. A. *J. Chem. Phys.* **2004**, *120*, 2677.
(4) Zundel, G. *Adv. Chem. Phys.* **2000**, *111*, 1.
(5) Yeh, L. I.; Okumura, M.; Myers, J. D.; Price, J. M.; Lee, Y. T. *J. Chem. Phys.* **1989**, *91*, 7319.
(6) Headrick, J. M.; Bopp, J. C.; Johnson, M. A. *J. Chem. Phys.* **2004**, *121*, 11523.
(7) Diken, E. G.; Headrick, J. M.; Roscioli, J. R.; Bopp, J. C.; Johnson, M. A.; McCoy, A. B. *J. Phys. Chem. A* **2005**, *109*, 1487.
(8) Hammer, N. I.; Diken, E. G.; Roscioli, J. R.; Johnson, M. A.; Myshakin, E. M.; Jordan, K. D.; McCoy, A. B.; Huang, X.; Bowman, J. M.; Carter, S. *J. Chem. Phys.* **2005**, *122*, 244301.
(9) McCunn, L. R.; Roscioli, J. R.; Johnson, M. A.; McCoy, A. B. *J. Phys. Chem. B* **2008**, *112*, 321.
(10) Devlin, J. P.; Severson, M. W.; Mohamed, F.; Sadlej, J.; Buch, V.; Parrinello, M. *Chem. Phys. Lett.* **2005**, *408*, 439.
(11) DeLuca, M. J.; Cyr, D. M.; Chupka, W. A.; Johnson, M. A. *J. Chem. Phys.* **1990**, *92*, 7349.
(12) Boucher, D. S.; Darr, J. P.; Bradke, M. D.; Loomis, R. A.; McCoy, A. B. *Phys. Chem. Chem. Phys.* **2004**, *6*, 5275.
(13) Honma, K.; Armentrout, P. B. *J. Chem. Phys.* **2004**, *121*, 8307.
(14) Ruoff, R. S.; Klots, T. D.; Emilsson, T.; Gutowsky, H. S. *J. Chem. Phys.* **1990**, *93*, 3142.
(15) Bosch, E.; Moreno, M.; Lluch, J. M. *J. Chem. Phys.* **1992**, *97*, 6469.
(16) Posey, L. A.; Johnson, M. A. *J. Chem. Phys.* **1988**, *89*, 4807.
(17) Robertson, W. H.; Kelley, J. A.; Johnson, M. A. *Rev. Sci. Instrum.* **2000**, *71*, 4431.
(18) Frisch, M. J.; Trucks, G. W.; Schlegel, H. B.; Scuseria, G. E.; Robb, M. A.; Cheeseman, J. R.; Montgomery, J. A., Jr.; Vreven, T.; Kudin, K. N.; Burant, J. C.; Millam, J. M.; Iyengar, S. S.; Tomasi, J.; Barone, V.; Mennucci, B.; Cossi, M.; Scalmani, G.; Rega, N.; Petersson, G. A.; Nakatsuji, H.; Hada, M.; Ehara, M.; Toyota, K.; Fukuda, R.; Hasegawa, J.; Ishida, M.; Nakajima, T.; Honda, Y.; Kitao, O.; Nakai, H.; Klene, M.; Li, X.; Knox, J. E.; Hratchian, H. P.; Cross, J. B.; Bakken, V.; Adamo, C.; Jaramillo, J.; Gomperts, R.; Stratmann, R. E.; Yazyev, O.; Austin, A. J.; Cammi, R.; Pomelli, C.; Ochterski, J. W.; Ayala, P. Y.; Morokuma, K.; Voth, G. A.; Salvador, P.; Dannenberg, J. J.; Zakrzewski, V. G.; Dapprich, S.; Daniels, A. D.; Strain, M. C.; Farkas, O.; Malick, D. K.; Rabuck, A. D.; Raghavachari, K.; Foresman, J. B.; Ortiz, J. V.; Cui, Q.; Baboul, A. G.; Clifford, S.; Cioslowski, J.; Stefanov, B. B.; Liu, G.; Liashenko, A.; Piskorz, P.; Komaromi, I.; Martin, R. L.; Fox, D. J.; Keith, T.; Al-Laham, M. A.; Peng, C. Y.; Nanayakkara, A.; Challacombe, M.; Gill, P. M. W.; Johnson, B.; Chen, W.; Wong, M. W.; Gonzalez, C.; Pople, J. A. *Gaussian 03*, revision C.02; Gaussian, Inc.: Wallingford, CT, 2004.
(19) Ojamae, L.; Shavitt, I.; Singer, S. J. *J. Chem. Phys.* **1998**, *109*, 5547.
(20) Huang, X.; Braams, B. J.; Bowman, J. M. *J. Chem. Phys.* **2005**, *122*, 044308.
(21) Walters, R. S.; Pillai, E. D.; Duncan, M. A. *J. Am. Chem. Soc.* **2005**, *127*, 16599.
(22) Johnson, M. A.; Rostas, J.; Zare, R. N. *Chem. Phys. Lett.* **1982**, *92*, 225.
(23) Brummer, M.; Kaposta, C.; Santambrogio, G.; Asmis, K. R. *J. Chem. Phys.* **2003**, *119*, 12700.
(24) Mikosch, J.; Kreckel, H.; Wester, R.; Plasil, R.; Glosik, J.; Gerlich, D.; Schwalm, D.; Wolf, A. *J. Chem. Phys.* **2004**, *121*, 11030.
(25) Engdahl, A.; Nelander, B. *J. Chem. Phys.* **1987**, *86*, 1819.
(26) Diken, E. G.; Shin, J.-W.; Price, E. A.; Johnson, M. A. *Chem. Phys. Lett.* **2004**, *387*, 17.
(27) Horvath, S.; McCoy, A. B.; Roscioli, J. R.; Johnson, M. A. In preparation.

JP802172Q